Effect of CeO$_2$ addition on crystallization behavior, bioactivity and biocompatibility of potassium mica and fluorapatite based glass ceramics

Ipek AKIN and Gultekin GOLLER[†]

Metallurgical and Materials Eng. Department, Istanbul Technical University, 34469 Maslak, Istanbul, Turkey

The bone-bonding ability of a glass ceramic can be evaluated by using simulated body fluid (SBF). Furthermore, rat primary osteoblast cell culture is effective in collecting preliminary information for potential application of any material of organic or inorganic origin. In this study, the effect of CeO$_2$ addition on crystallization behavior and bioactivity of potassium mica and fluorapatite based glass ceramics was investigated. Also an osteoblast cell culture model was utilized to investigate the effect of CeO$_2$ addition on biocompatibility of potassium mica and fluorapatite based glass ceramics by using biological criteria such as cell viability, metabolic activity and nitric oxide production.

1. Introduction

Machinable glass ceramics, which are applied to orthopedic and dental applications, especially in the replacement of natural bone and dental restoration, are greatly important due to the development of controlled nucleation and crystallization of the glass ceramics.[1)–4)] Mica-containing glass-ceramics provide machinability. That is, they can be machined, cut, or drilled with normal metalworking tools. Their machinability results in an increased versatility of the products and numerous possibilities of industrial applications. The excellent machinability of mica glass ceramics results from the cleavage of interlocking layers of mica (phlogopite) crystals precipitated in the glass matrix. The precipitated mica phase must constitute more than two-thirds of the total volume for an effective machinability.[5)–10)]

For a material to be machinable and bioactive, it should contain both mica and apatite crystals. Apatite containing glass ceramics are greatly important for surgical implantation due to the high bioactivity, close crystallographic and chemical similarity to human bone tissue.[11)–14)] The crystalline phases occurring in these glass ceramics include essentially apatite which provides the biocompatibility and bioactivity of the glass ceramics, and mica, secondary crystalline phase, crystallized at higher temperature and provides the interesting mechanical properties such as machinability, hardness and strength.[11)–13)]

In the production of glass ceramics, nucleating agents such as CeO$_2$, TiO$_2$ or ZrO$_2$ can be used in order to induce bulk crystallization of the phases. Furthermore, the addition of nucleating agents to the main glass can decrease the crystallization time and temperature.[15),16)] In a previous study, Goller et al. has investigated the crystallization behavior of mica and fluorapatite based glass ceramics as a function of TiO$_2$ addition. According to the microstructural investigations and machinability test results, optimum TiO$_2$ addition was determined as 1 wt%.[17)] In another study, Leonelli et al. has investigated the in-vitro bioactivity

behavior of phosphosilicate glasses based on Bioglass® 45S5 doped with cerium oxide (CeO$_2$).[18)] They reported that, the choice of CeO$_2$ was related to its low toxicity and good bacteriostatic properties. In addition, cerium doped bioactive glasses can be useful when implantation concerns local infected areas.[18)] No open literature about the effect of CeO$_2$ addition as a nucleation agent on crystallization behavior of the mica based glass ceramics has been published.

The purpose of this study is to investigate the effect of CeO$_2$ addition on the crystallization behavior, microstructural morphology, machinability and bioactivity of the glass ceramics having 3:7 weight ratio of fluorapatite to potassium mica. Also an osteoblast cell culture model system was utilized to investigate the effect of CeO$_2$ addition on biocompatibility by using biological criteria such as cell viability, metabolic activity and nitric oxide production.

2. Experimental procedure

2.1 Glass ceramic production and characterization

The reagents (Merck) of SiO$_2$, MgO, P$_2$O$_5$, Al$_2$O$_3$, K$_2$CO$_3$, CaCO$_3$, and CaF$_2$ were used as starting materials of glass ceramics having 3:7 weight ratio of fluorapatite (Ca$_{10}$(PO$_4$)$_6$F$_2$) to potassium mica (K$_2$Mg$_3$AlSi$_3$O$_{10}$F$_2$). CeO$_2$ was added to the compositions as nucleating agent. The raw materials were mixed for 2 h and then calcined powders were melted in a sealed platinum crucible at 1400°C for 1 h and then quenched into the water. Differential thermal analysis (DTA, Perkin Elmer Diamond TG/DTA) measurements were performed for each glass composition under nitrogen atmosphere. The DTA scan rate was 0.16°C/s and glass powders were heated up to 1000°C. In order to determine crystalline phases, the heat treated glass ceramic samples were subjected to X-ray diffraction analysis (XRD; Rigaku Miniflex) by employing Cu Kα radiation and in the 2θ range from 10° to 80°.

Disc and cylindrical shaped samples were prepared by using casting method in order to determine microstructural and mechanical properties of the glass ceramics. The melted glass

---

† Corresponding author: G. Goller; E-mail: goller@itu.edu.tr

JCS-Japan

Akin et al.: Effect of CeO₂ addition on crystallization behavior, bioactivity and biocompatibility of potassium mica and fluorapatite based glass ceramics

was poured into the preheated graphite moulds and the as-cast glasses were immediately put into in a furnace for annealing. After that, controlled heat treatment programme was applied for glass ceramic production. Proper heat treatment conditions were determined as a result of heat treatment and XRD measurement cycle. Possible nucleation and crystallization temperatures were obtained from DTA results and several heat treatments were applied. Heat treated glasses were characterized by X-ray diffraction and proper heat treatment temperatures were determined according to the formation of potassium mica and fluorapatite. The glass ceramic samples, after polishing (1 μm diamond slurry) and etching in 5 vol% HF solution for 20–30 s, were coated with a thin film gold and subjected to microscopic examination by a field emission scanning electron microscope (FE–SEM; JEOL Ltd., JSM–7000F). Microhardness tests were applied to the polished samples under constant load of 9.8 N with 12 s indentation time. Machinability tests were subjected to the disc shaped specimens by using 5 mm diamond drills with 710 rpm drilling rate under water cooling and uncontrolled load. The glass compositions with no additive, 1 and 2 wt% CeO₂ additions have designated as C0, C1, and C2, respectively.

2.2 Simulated body fluid (SBF)

The specimens C0 and C1 were soaked in simulated body fluid, with ion concentrations nearly equal to those of human blood plasma. SBF was prepared by using appropriate quantities of NaCl, NaHCO₃, KCl, K₂HPO₄.3H₂O (99%), MgCl₂.6H₂O (99.7%), CaCl₂ (99.6%), Na₂SO₄ and NH₂C(CH₂OH)₃ (100%) were dissolved in deionized water and buffered with 1N hydrochloric acid (HCl) at pH 7.4 and the temperature of the solution was adjusted as 36.5°C. In-vitro tests were performed under dynamic conditions, approximately 80 rpm, under nitrogen atmosphere. Samples were removed from the solution after 1 h, 1, 7, 14, 21 and 28 d. The morphology of the precipitation apatite layer on the surface depending on time and nucleating agents, and microstructures of the samples were examined by using FE–SEM.

2.3 Osteoblast cell culture

Osteoblasts were isolated from the calvaria of 1–3 d old neonatal Wistar rats. The calvaria were dissected and removed from the soft tissue, cut into small pieces and rinsed in sterile phosphate-buffered saline without calcium and magnesium. The calvaria pieces were incubated with 1% trypsin-EDTA for 300 s, followed by five sequential incubations with 0.2% collagenase at 37°C for 1.8×10^3 s each. The supernatant of the first collagenase incubation, which contain a high proportion of periosteal fibroblasts, were discarded. The other digestions produced a suspension of cells with high proportion of osteoblasts. After centrifugation at 3000 g for 300 s, each pellet were resuspended in 5 ml of RPMI medium supplemented with 10% FBS, 1% antibiotic-antimycotic. The cells were seeded into 250 ml tissue culture flasks, and led to grow in a controlled 5% CO₂, 95% humidity incubator at 37°C.

Following cell proliferation on the cell culture flask, cells were splitted from the surface by applying 1 ml of 1% trypsin. Cells were resuspended in 15 ml of culture medium and osteoblast cells were used to seed 12 well plates. 500 μl of cell suspension were added into each well and allowed to settle for 24 h. Following settling of the cells at the bottom of the flask, materials (one into each well) were added and following the 72 h of incubation at 37°C in RPMI–1640 medium with 5% CO₂ and 95% humidity, proceeded with the assays.

C0 glass ceramics nucleated at 610°C for 1 h and crystallized

at 770°C for 4 h, C1 and C2 glass ceramics nucleated at 610°C for 1 h and crystallized at 750°C for 3 h were characterized in terms of cell viability, alkaline phosphatase activity and nitric oxide production.

2.3.1 Cell viability

After 72 h of incubation in the presence of different types of samples, osteoblast viability was evaluated by MTT assay, based on the reduction of tetrazolium salt to formazan crystals by living cells. About 60 μl of MTT (5 mg/ml) was added to each well. After incubation for 24 h the optical density measurement was done at 570 nm.

2.3.2 Alkaline phosphatase activity

The alkaline phosphatase production was evaluated by BCIP–NBT assay. This assay is based on achromagenic reaction initiated by the cleavage of the phosphate group of BCIP by alkaline phosphatase present in the cells. This reaction produces a proton, which reduces NBT to an insoluble purple precipitate. After 2 h of incubation, the insoluble purple precipitates were solubilized with 210 μl of SDS 10% HCl and incubated for 24 h. The optical density measurement was done at 595 nm.

2.3.3 Nitric oxide measurement

Osteoblast nitric oxide production was indirectly measured by supernatant nitrite quantification, since it is one of two primary stable and nonvolatile breakdown products of NO. Griess assay was used, which relies on a diazotization reaction among 1% sulfanilamide, 0.1% naphhthylene diamine in 2.5% phosphoric acid and nitrite. This reaction forms a chromophore. A volume of 50 μl of reagent was mixed to 50 μl of each culture supernatant. After 1.8×10^3 s, the absorbance reading, at 540 nm, showed the total level of nitrite in each sample and the concentration was calculated by means of NaNO₂ standard curve. Assay was performed for nitrite measurement in the cultures supernatants and in the media without cells.

3. Results and discussion

3.1 DTA and XRD results

According to DTA results, all compositions showed double endothermic peaks indicating the formation of phase separation. The glass transition (T_g) and crystallization (T_c) temperatures of the glasses are listed in **Table 1**. According to the overall DTA results, CeO₂ addition decreased the crystallization temperatures of the glasses. This could be attributed reducing of the number of bridging bonds in the silica-based network and leading to a decrease of the viscosity and promoted crystallization of the glass. Hu et al. prepared LiO₂–Al₂O₃–SiO₂ glass system with 5 wt% CeO₂ and reported that crystallization temperature decreased from 872°C to 851°C with the addition of CeO₂.[19] On the other hand, addition of CeO₂ increased the glass transition temperatures of the C1 and C2 glasses. El-Damrawi and El-Egili studied the CeO₂–B₂O₃ glasses and investigated that glass transition temperature of the system increased with increasing CeO₂ content.[20] CeO₂ can play a dual role, as both a network former and network modifier. The structure of silicate, aluminosilicate

Table 1. Glass Transition (T_g) and Crystallization Temperatures (T_c) of Glasses

	Glass		
	C0	C1	C2
T_g (°C)	584	600	598
T_c (°C)	751	742	748

and phosphate glasses containing CeO_2 has been investigated and results showed that cerium ions can act as glass modifiers forming non-bridging oxygen atoms in the silicate network and also it can be network former due to the fraction of 4-coordinated cerium atoms, CeO_4.[20]–[22] Same results were reported for the phosphate glasses.[20] Higher glass transition temperatures can be caused due to the addition of CeO_2 acted as a network former.

According to the XRD results (**Fig. 1**), it was observed that, potassium mica (JPDS 16–0352) and fluorapatite (JPDS 15–0876) were crystallized simultaneously for the compositions of C0 nucleated at 610°C for 1 h and crystallized at 770°C for 4 h and C1 samples nucleated at 610°C for 1 h and crystallized at 750°C for 3 h . However, the XRD patterns of the C2 glass ceramic showed only the formation of fluorapatite. It should be noted that the crystallization of potassium mica was impeded by the addition of 2 wt% CeO_2.

3.2 Microstructural characterization

Microstructures of polished surfaces of C0 glass ceramics nucleated at 610°C for 1 h and crystallized at 770°C for 4 h, C1 glass ceramics heat treated at 610°C for 1 h and 770°C for 4 h, and 750°C for 3 h are given in **Fig. 2**. For C0 glass-ceramics, at 770°C plate-like fluorapatite crystals with size of 2–4 μm were formed. Potassium mica crystals of 4–5 μm in width formed an interlocking structure. In the microstructures of C1 glass ceramics nucleated at 610°C for 1 h and crystallized at 750°C for 3 h and 770°C for 4 h, homogeneously distributed fluorapatite crystals with a size of 4–5 μm were observed.

3.3 Mechanical characterization

Microhardness is a key parameter for machinability of glass ceramics. The overall microhardness results are given in **Table 2**. According to the microhardness test results, the proper controlled heat treatment process for machinability of C0 glass ceramics was determined as nucleated at 610°C for 1 h and crystallized at 770°C for 4 h. For C1 composition, the proper nucleation and crystallization heat treatment process was determined as nucleation at 610°C for 1 h and crystallized at 750°C for 3 h. The data in Table 2 also indicate that the CeO_2-containing glass

ceramics have higher Vickers microhardness when compared with C0 glass ceramics. An increase in glass transition temperature with the addition of CeO_2 resulted in increasing microhardness of glass ceramics. This may be explained by the strength and nature of the bonds governed by the addition of CeO_2 and resulted in an increasing compactness of the glass network.

The machinability of heat treated disc shaped specimens of compositions C0 and C1 was tested and compared with each other. The disc shaped specimen of C0 glass ceramic nucleated at 610°C for 1 h and crystallized at 770°C for 4 h showed excellent machinability and a 10 mm thick hole was drilled successfully without cracking in 210 s. The samples of C1 glass ceramics that nucleated at 610°C for 1 h and crystallized at 750°C for 3 h showed excellent machinability and completely 8–10 mm thick holes were drilled without cracking in 300 s.

Fig. 2. SEM micrographs of (a) C0 specimen nucleated at 610°C for 1h and crystallized at 770°C for 4 h, (b) C1 specimen nucleated at 610°C for 1 h and crystallized at 770°C for 4 h, (c) C1 specimen nucleated at 610°C for 1 h and crystallized at 750°C for 3 h.
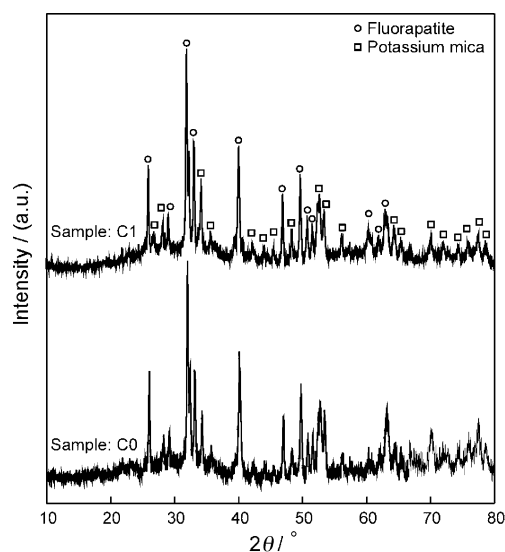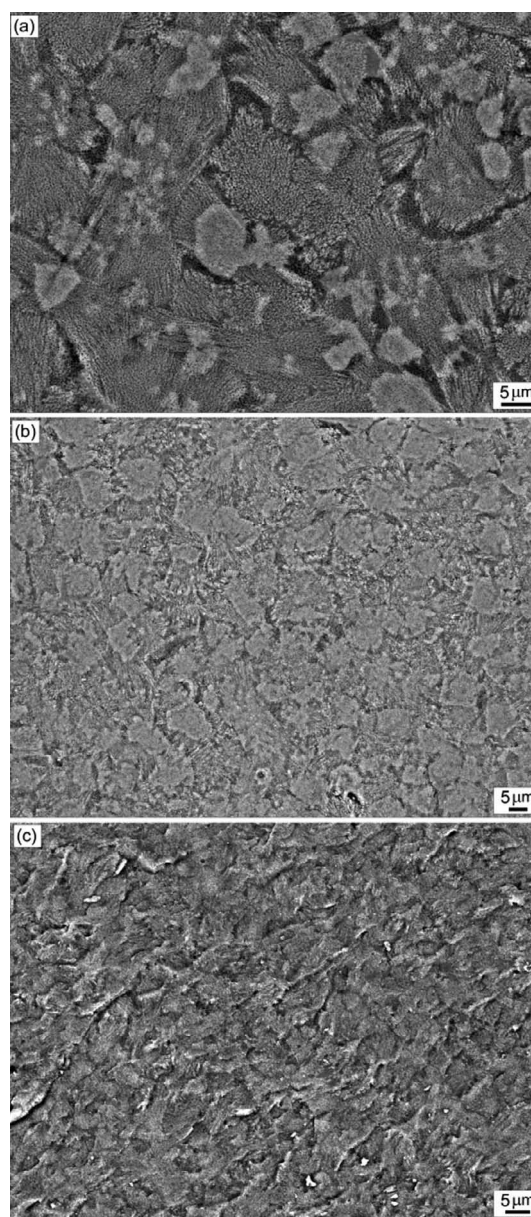

Fig. 1. XRD results of C0 glass ceramics nucleated at 610°C for 1 h and crystallized at 770°C for 4 h, and C1 glass ceramics nucleated at 610°C for 1 h and crystallized at 750°C for 3 h.

JCS-Japan

Akin et al.: Effect of CeO₂ addition on crystallization behavior, bioactivity and biocompatibility
of potassium mica and fluorapatite based glass ceramics

Table 2. Microhardness Test Results of C0 and C1 Glass Ceramics

	Heat Treatment	Microhardness (GPa)
C0	600°C/1 h + 770°C/3 h	4.64 ± 0.21
	600°C/1 h + 770°C/4 h	4.35 ± 0.19
	610°C/1 h + 770°C/3 h	4.41 ± 0.17
	610°C/1 h + 770°C/4 h	5.01 ± 0.22
C1	600°C/1 h + 750°C/3 h	5.29 ± 0.21
	600°C/1 h + 750°C/4 h	5.21 ± 0.19
	610°C/1 h + 750°C/3 h	5.13 ± 0.20
	610°C/1 h + 750°C/4 h	5.18 ± 0.16
	600°C/1 h + 770°C/3 h	5.30 ± 0.23
	600°C/1 h + 770°C/4 h	5.22 ± 0.20
	610°C/1 h + 770°C/3 h	5.21 ± 0.18
	610°C/1 h + 770°C/4 h	5.18 ± 0.23

3.4 Simulated body fluid (SBF)

The in-vitro bioactivity test results of glass ceramics without CeO₂ addition have been reported in a previous study.[23] The microstructural investigations of C1 glass ceramics nucleated at 610°C for 1 h and crystallized at 750°C for 3 h are given in **Fig. 3**. The Ca–P precipitation was observed after 7 d immersion in SBF as indicated with white arrows in Fig. 3(a). Precipitation started at individual particles and plate-like crystals with size of 0.5–1 μm formed. After 14 d, the morphology of plate-like crystals changed and lath-like crystals (0.5 μm in width and 1–1.5 μm in length) started to form on the surface as shown in Fig. 3(b). These lath-like crystals gradually grew in size (1–2 μm in width and 6–8 μm in length) and formed a dense layer on the glass ceramics surfaces at the end of the 21 d after immersion in SBF (Fig. 3(c)). After 28 d, dense and continuous biological apatite layer with a thickness of 5–8 μm was observed and given in Fig. 3(d) as a cross-section micrograph image.

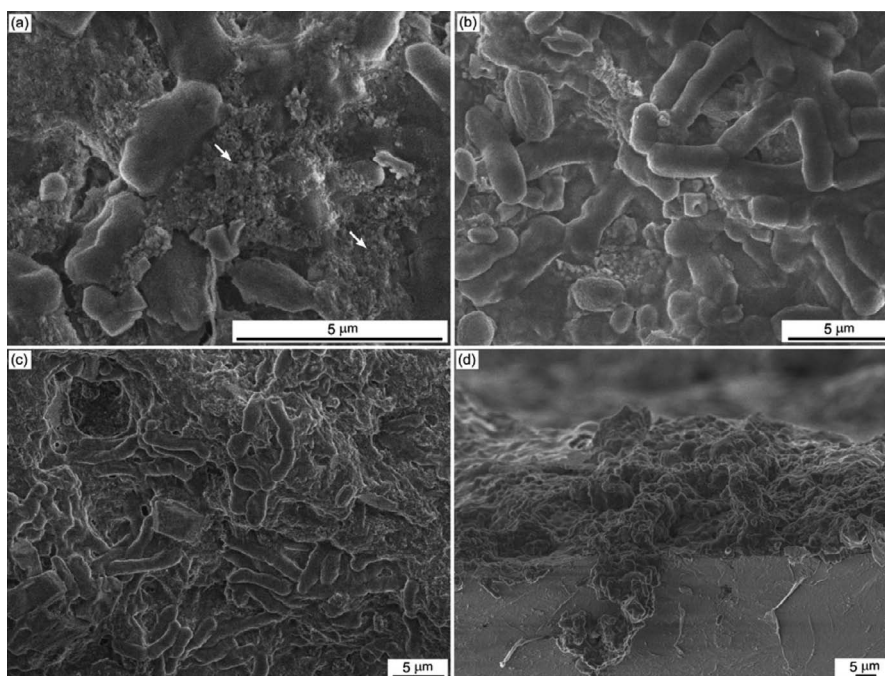**Figure 4** shows the thin film XRD (TF–XRD) analysis of C0

Fig. 3. SEM micrographs of C1 glass-ceramic samples (a) after 7 d of immersion in SBF, (b) after 14 d of immersion in SBF, (c) after 28 d of immersion in SBF, (d) crosssection micrograph at the end of the 28 d.
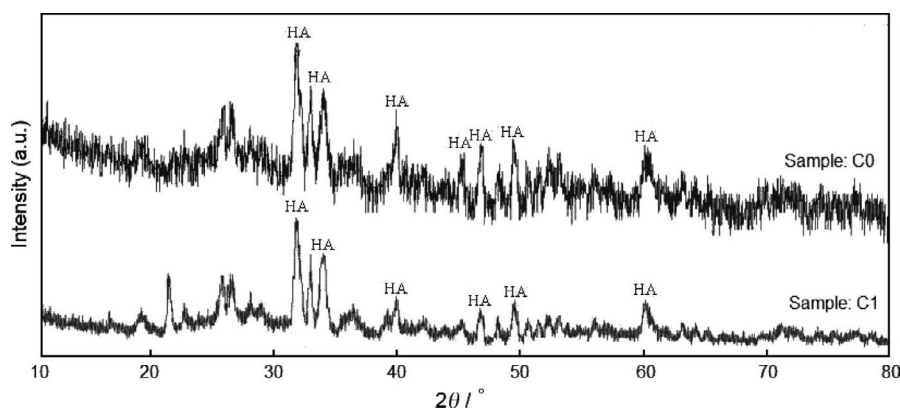

Fig. 4. TF–XRD results of (a) C0 glass ceramics nucleated at 610°C for 1 h and crystallized at 770°C for 4 h, (b) C1 glass ceramics nucleated at 610°C for 1 h and crystallized at 750°C for 3 h after immersion in SBF 28 d (HA: hydroxyapatite).
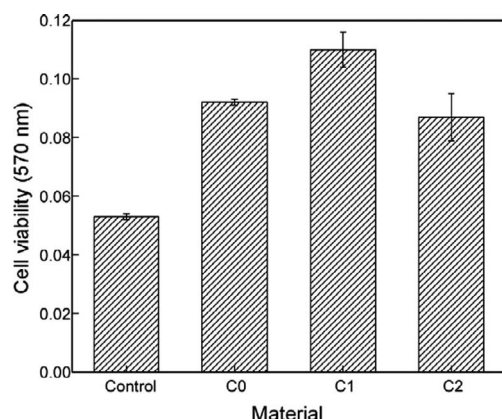
Fig. 5. Cell viability results of C0 glass ceramics heat treated at 610°C/1 h + 770°C/4 h, C1 and C2 glass ceramics heat treated at 610°C/1 h + 750°C/3 h.
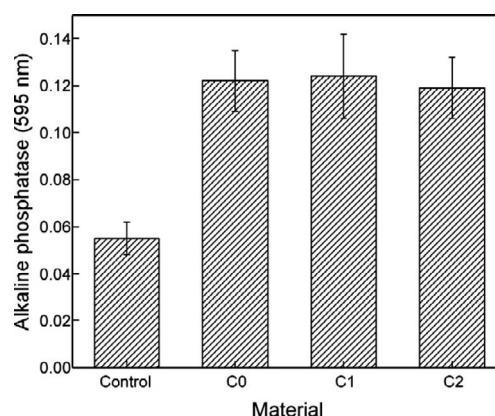

Fig. 6. Alkaline phosphatase activity C0 glass ceramics heat treated at 610°C/1 h + 770°C/4 h, C1 and C2 glass ceramics heat treated at 610°C/1 h + 750°C/3 h.

glass ceramics nucleated at 610°C for 1 h and crystallized at 770°C for 4 h, and C1 glass ceramics nucleated at 610°C for 1 h and crystallized at 750°C for 3 h after 28 d of immersion in SBF. TF–XRD results indicated that after precipitation of initial crystals, crystallization proceeded and crystallization of precipitated hydroxyapatite (JPDS 01–1008) appeared after soaking for 28 d. Although the peaks of hydroxyapatite and fluorapatite are very similar, it is possible to conclude that, the peaks corresponding to potassium mica disappeared and the formation of apatite on the surfaces of glass-ceramics was achieved at the end of the 28 d. Also, the SEM studies given in Fig. 3 showed a consistency with XRD results about the formation of apatite.

3.5 Osteoblast cell culture

The results of cell viability, alkaline phosphatase activity and nitric oxide production of C0 glass ceramics nucleated at 610°C for 1 h and crystallized at 770°C for 4 h, C1 and C2 glass ceramics nucleated at 610°C for 1 h and crystallized at 750°C for 3 h are given in **Figs. 5–7**. The cell viability was not prevented by the presence of the glass ceramics; in contrast, it was slightly enhanced. Thus, glass ceramics stimulate osteoblast activity. Alkaline phosphatase production by the osteoblasts is an indication of biological activity of these cells because growing bones need alkaline phosphatase. Results indicated that materials did not impede alkaline phosphatase production, besides it was slightly induced. This is another indication that the osteoblasts continue their physical functions normally in the presence of glass ceramics. The NO production may be an indication of the early bone mineralization, or homeostatic and development functions or immune response of the mammalian cells. There is no significant effect of material on NO production. Andrade et al. has studied the in vitro bioactivity and biocompatibility of fiber and bulk bioactive glasses produced by sol–gel method.[24] They have reported that osteoblast viability decreased 60% in the presence of fiber glass and 20% in the presence of bulk glass when compared to control group. They have explained the poor cell viability by the morphology of the materials and fiber dimensions. Valerio et al. has investigated the behavior of osteoblast cells in the presence of a bioactive glass with 60% of silica produced by sol–gel process and a biphasic calcium phosphate.[25] They observed that osteoblast proliferation was 35% higher in the presence of ionic products from the dissolution of bioactive glass with 60 wt% of silica and they found that this type of
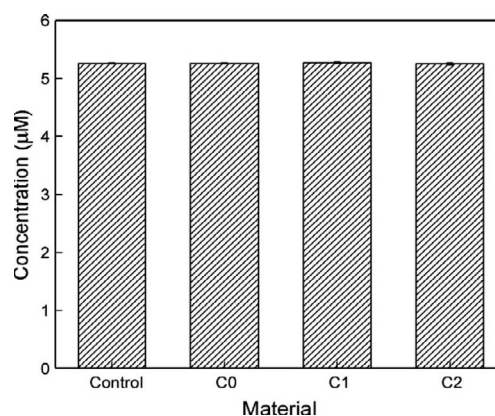

Fig. 7. Nitric oxide production of C0 glass ceramics heat treated at 610°C/1 h + 770°C/4 h, C1 and C2 glass ceramics heat treated at 610°C/1 h + 750°C/3 h.

bioactive glass acted as an NO donor. Silicic acid release also enhanced the collogen type I production. These results show that the morphology of the materials influence their physiological performance. The slightly enhancement of osteoblast activity for C1 glass ceramics may be attributed to the release of silica. It may have caused by the addition of 1 wt% CeO_2 acted as a network former because highest glass transition temperature was observed for this composition, and changed the silica network, and higher amount of silica released. Oonishi et al.,[26] Wilson et al.[27] and Feng et al.[28] reported that bioglass implants have osteoproductive qualities. These kinds of materials do not simply serve as a scaffold for bone formation but seem to improve osteoblast activity due to the slow release of silicon produced as the graft particles is consumed and then promotes an autocrine response with enhancement of osteoblast activity.

4. Conclusions

Addition of CeO_2 as a nucleating agent decreases the crystallization temperature of the glasses up to 1.5 wt%. When the addition of CeO_2 exceeds 1.5 wt%, crystallization temperatures of the glasses slightly shifted to higher temperatures. In addition, when the CeO_2 content is increased to 1.5 wt%, potassium mica formation is reduced and some CeO_2 crystals begin to form.

The simulated body fluid and osteoblast cell culture tests

JCS-Japan

Akin et al.: Effect of CeO₂ addition on crystallization behavior, bioactivity and biocompatibility
of potassium mica and fluorapatite based glass ceramics

showed that potassium mica-fluorapatite glass ceramics with and without CeO_2 addition have good biocompatibility and bioactivity. The apatite formation was observed for glass ceramics and according to the microstructural investigations; addition of 1 wt% CeO_2 changed the morphology of precipitated apatite layer. Lath-like apatite formed on the surface. In the biological response studies, there was no any unaccepted observation for the glass ceramics containing varying amount of ceria. Glass ceramics stimulated osteoblast activity, i.e. cell viability and alkaline phosphatese activity, and having 1 wt% CeO_2 are even better off cell viability. It may be attributed to addition of CeO_2 acted as a network former and changed the silica network, and higher amount of silica released. Nitric oxide production was not affected by the presence of glass ceramics and CeO_2 addition as desired.

References

1) S. Jordery, W. Lee and P. F. James, *J. Am. Ceram. Soc.*, **81**, 2237–2244 (1998).
2) J. J. Shyu and J. M. Wu, *J. Mater. Sci. Lett.*, **10**, 1056–1058 (1991).
3) X. Chen, L. L. Hench, D. Greenspan, J. Zhong and X. Zhang, *Ceram. Int.*, **24**, 401–410 (1998).
4) J. M. Tzeng, J. G. Duh, K. H. Chung and C. C. Chan, *J. Mater. Sci.*, **28**, 6127–6135 (1993).
5) D. S. Baik, K. S. No and J. S. Chun, *J. Am. Ceram. Soc.*, **78**, 1217–1222 (1995).
6) P. W. McMillan, "Glass-Ceramics," Second ed., Academic Press, London (1979) pp. 31–44.
7) W. Vogel, W. Höland, K. Naumann and J. Gummel, *J. Non-Cryst. Solids*, **80**, 34–51 (1986).
8) H. Rawson, "Properties and Applications of Glass," First ed., Elsevier, Amsterdam (1980) pp. 48–89.
9) T. Uno, T. Kasuga and K. Nakajima, *J. Am. Ceram. Soc.*, **74**, 3139–3141 (1991).
10) J. L. Xie, H. Feng and S. Wenhua, *Glass. Technol.*, **37**, 175–178 (1996).
11) L. Rounan and Z. Peinan, *J. Non-Cryst. Solids*, **80**, 600–604 (1986).
12) H. A. Elbatal, M. A. Azooz, E. M. A. Khalil, A. S. Monem and Y. M. Hamdy, *Mater. Chem. Phys.*, **80**, 599–609 (2003).
13) W. Höland, W. Vogel, K. Naumann and J. Gummel, *J. Biomed. Mater. Res.*, **19**, 303–312 (1985).
14) W. Vogel and W. Höland, *Angew. Chem. Int. Ed. Engl.*, **26**, 527–544 (1987).
15) W. Vogel, "Glass Chemistry," Springer-Verlag, Berlin (1994) pp. 91–103.
16) C. L. Lo, J. G. Duh, B. S. Chiou and W. H. Lee, *Mater. Res. Bull.*, **37**, 1949–1960 (2002).
17) I. Akin and G. Goller, *J. Mater. Sci.*, **42**, 883–888 (2007).
18) C. Leonelli, G. Lusvardi, G. Malavasi, L. Menabue and M. Tonelli, *J. Non-Cryst. Solids*, **316**, 198–216 (2003).
19) A. M. Hu, K. M. Liang, F. Zhou, G. L. Wang and F. Peng, *Ceram. Int.*, **31**, 11–14 (2005).
20) G. El-Damrawi and K. El-Egili, *Physica B*, **299**, 180–186 (2001).
21) S. L. Lin and C. S. Hwang, *J. Non-Cryst. Solids*, **202**, 61–67 (1996).
22) Y. Y. Ivanova, E. J. Spassova, E. P. Kashchieva, M. A. Bursukova and Y. B. Dimitriev, *J. Non-Cryst. Solids*, **192–193**, 674–678 (1995).
23) G. Goller, I. Akin, N. Eruslu and E. S. Kayali, *Key Eng. Mater.*, **309–311**, 321–324 (2006).
24) A. L. Andrade, P. Valerio, A. M. Goes, M. F. Leite and R. Z. Domingues, *J. Non-Cryst. Solids*, **352**, 3505–3511 (2006).
25) P. Valerio, M. M. Pereria, A. M. Goes and M. F. Leite, *Biomaterials*, **25**, 2941–2948 (2005).
26) H. Oonishi, S. Kushitani, E. Yasukawa and H. Iwaki, *Clin. Orthop.*, **364**, 316–325 (1997).
27) J. Wilson, S. Low and A. Fetner, *Biomaterials and Clinical Applications*, **8**, 223–228 (1987).
28) Y. Z. Feng, W. Wang, Y. Tan, Y. Liu, Q. Xian and X. Sheng, *Trans. Nonferrous Met. Soc. China*, **17**, 828–831 (2007).